ERDC/EL TR-15-8

US Army Corps of Engineers®
Engineer Research and Development Center

ERDC
INNOVATIVE SOLUTIONS for a safer, better world

Ecosystem Management and Restoration Research Program

Kinetics Formulations for ICM-Lite: A Tool to Predict and Quantify Ecosystem Benefits in Aquatic Systems

Carl F. Cerco

July 2015

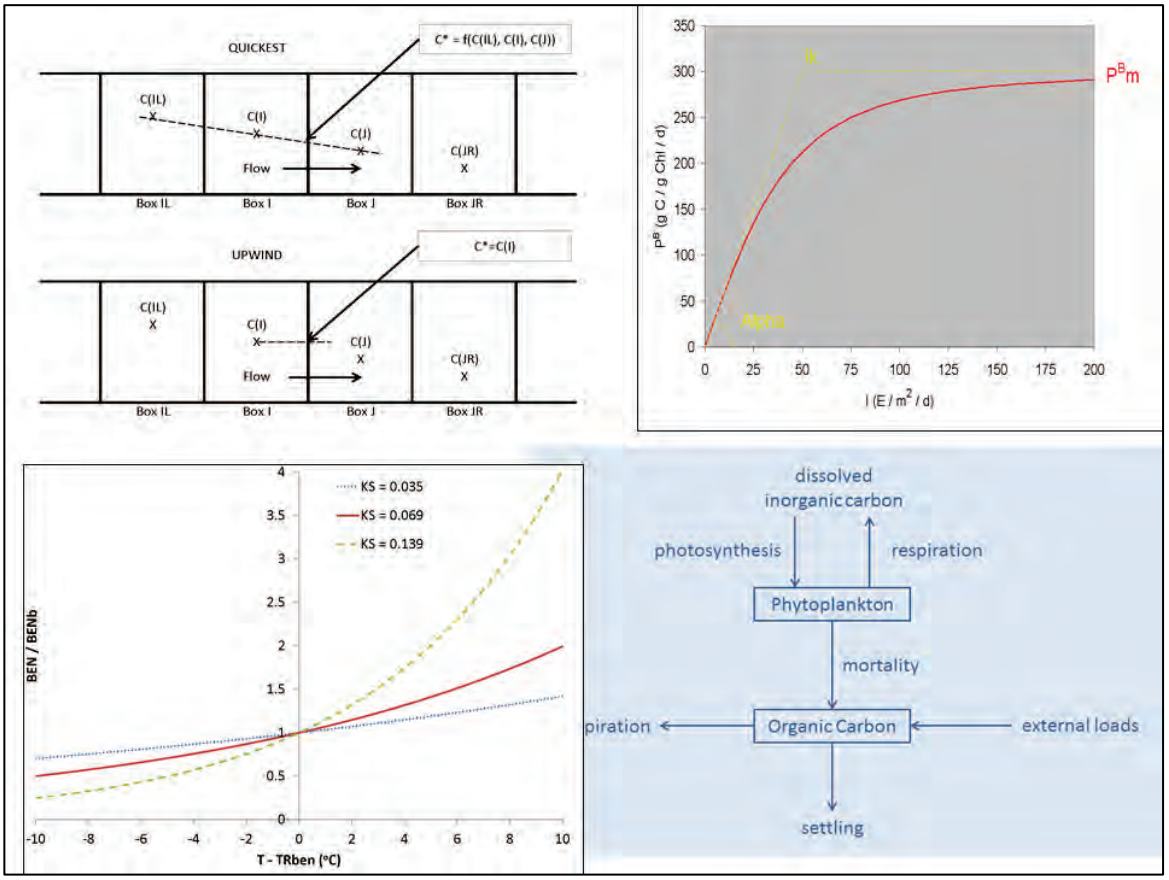

Environmental Laboratory

The U.S. Army Engineer Research and Development Center (ERDC) solves the nation's toughest engineering and environmental challenges. ERDC develops innovative solutions in civil and military engineering, geospatial sciences, water resources, and environmental sciences for the Army, the Department of Defense, civilian agencies, and our nation's public good. Find out more at www.erdc.usace.army.mil.

To search for other technical reports published by ERDC, visit the ERDC online library at http://acwc.sdp.sirsi.net/client/default.

Ecosystem Management and Restoration
Research Program

ERDC/EL TR-15-8
July 2015

Kinetics Formulations for ICM-Lite: A Tool to Predict and Quantify Ecosystem Benefits in Aquatic Systems

Carl F. Cerco

Environmental Laboratory
U.S. Army Engineer Research and Development Center
3909 Halls Ferry Road
Vicksburg, MS 39180

Final report

Prepared for U.S. Army Corps of Engineers
Washington, DC 20314-1000

Abstract

ICM-Lite is envisioned as a tool to rapidly predict and quantify ecosystem benefits in aquatic systems. ICM-Lite consists of three modules: a water quality module, a graphical user interface, and an ecosystems benefits module. This publication documents the formulations of the water quality module. Documentation includes the mass balance equation, kinetics in the water column, and representations of sediment-water fluxes. The mass balance relationships are intended to incorporate flows and volumes provided by the user and obtained outside of ICM-Lite. The kinetics include representations of the aquatic carbon, nitrogen, phosphorus, and oxygen cycles. Salinity, temperature, suspended solids, and one user-defined substances are included, as well. Sediment-water fluxes of organic matter, ammonium, nitrate, phosphate, and dissolved oxygen are considered.

Contents

Figures and Tables

Figures

Tables

Preface

This study was conducted for the Ecosystem Management and Restoration Research Program (EMRRP) as "A Tool to Rapidly Predict and Quantify Ecosystem Benefits." The USACE proponent for the EMRRP is Mindy Simmons. The Technical Director is Dr. Al Cofrancesco, and Program Manager is Glenn Rhett.

The report was prepared by Dr. Carl F. Cerco of the Water Quality and Contaminant Modeling Branch (WQCMB), Environmental Laboratory (EL), U.S. Army Engineer Research and Development Center (ERDC). The report was prepared under direct supervision of Dr. Dorothy Tillman, Branch Chief, WQCMB; under the general supervision of Warren Lorentz, Division Chief, Environmental Processes and Engineering Division; and Dr. Beth Fleming, Director, EL, ERDC.

At the time of publication, LTC John T. Tucker III was Acting Commander. Dr. Jeffery Holland was ERDC Director.

1 Introduction

1.1 The problem

The U.S. Army Corps of Engineers (USACE) needs to quantify ecosystem benefits to organisms and to the aquatic environment that result from USACE restoration projects. The USACE presently operates a number of predictive hydrodynamic and water quality models which compute environmental properties such as water temperature, water clarity, and dissolved oxygen. While these tools are superb, their applicability can be limited in the present operational climate. One limitation is their complexity. The existing models provide results at high levels of spatial and temporal resolution by employing detailed representations of physical and biogeochemical processes. The production of results at these levels of detail requires large volumes of data, for setup and validation, and extensive time for application by skilled specialists. These resource demands result in corresponding high costs. Both the time and the cost weigh against the current trends in planning as expressed, for example, in the recent "3x3x3" directive (Walsh 2012).

Resource requirements, especially time, comprise a second limitation to the utility of current planning models. They are ill suited for uncertainty analysis. Multiple approaches to quantifying uncertainty associated with ecosystem benefits are available but all share in common the need to execute and analyze large numbers of model runs based on varying input parameter sets. The time involved to set up, execute, and analyze results from the current suite of predictive tools precludes their employment in Monte Carlo analyses and other examinations of uncertainty.

An additional limitation in existing planning tools is inherent in the nature of the information produced. The current models provide basic physical properties, such as temperature or turbidity, at locations and times determined by model time-step and computational grid. The information desired, however, is often characterized in terms of ecosystem benefits or habitat suitability expressed in units and over spatial and temporal scales that are not explicit in the model computational details.

The USACE will always have projects that demand the state-of-the-art in high-fidelity planning models. Clearly, however, the USACE also requires a simpler tool (or tools) with the following characteristics:

- fast and easy to apply
- capable of uncertainty analysis
- applicable at the District level by nonspecialists
- results provided in useful and immediately understandable terms.

1.2 This study

The present study consists of three phases:

- reduce the complexity of a popular USACE planning tool to rapidly provide basic results
- wrap the simplified tool in a graphical interface (GUI) to facilitate use at the District level
- enable the GUI to conduct uncertainty analyses and to provide output in desired terms.

The USACE ERDC is the creator and operator of the Corps of Engineers Water Quality Integrated Compartment Model (CE-QUAL-ICM or simply ICM). This state-of-the-art model has been employed in lakes, rivers, and estuaries throughout the United States and overseas. The model is subject to the limitations noted above, however. ICM requires experienced users and can be expensive and time consuming to apply. The initial phase of this project will create an ICM-Lite, a simplified version of ICM kinetics. ICM-Lite will compute aquatic properties including salinity, temperature, dissolved oxygen, chlorophyll, total suspended solids, and turbidity. ICM-Lite is envisioned for an aquatic system that is represented by one well-mixed cell or by a simple network of cells. Basic hydrodynamics will be based on flows and exchange coefficients.

The second phase of the project will be the development of a GUI that will facilitate ICM-Lite application by the novice user. Both GUI and model will operate on a Windows PC. The GUI is envisioned to prompt the user for desired information and to suggest default values when these are appropriate. Habitat criteria or similar information input to the GUI by the user will be employed to translate the native information produced by the model, such as dissolved oxygen, into ecosystem benefits or other useful terms.

The swift execution of ICM-LITE will allow for Monte Carlo simulations and uncertainty analysis. The GUI will provide built-in guidance for this process. As a result, ecosystem benefits and/or restoration of desirable habitat can be expressed as an expected range of values along with associated probabilities.

1.3 This report

The project plan calls for the first project year to be devoted to reducing the existing CE-QUAL-ICM from its present 30+ state variables to a suite of 8 to 10, including basic physical properties such as temperature and salinity, nutrients, dissolved oxygen, and chlorophyll. The present report details the formulation of the new ICM-Lite.

2 The Conservation of Mass Equation

2.1 The model grid

Application of the model requires division of the study system into a grid of discrete volumes or cells. Although each volume is three-dimensional, the grid may be one-, two-, or three-dimensional (1D, 2D, 3D), depending on the arrangement of the cells. An example of a 2D grid is shown as Figure 1. This grid contains ten cells in the longitudinal dimension, one cell in the lateral dimension, and three cells in the vertical dimension.

Figure 1. Example of 2D grid (elevation). The grid is ten cells in the longitudinal direction, three cells in the vertical direction, and one cell in the lateral direction.

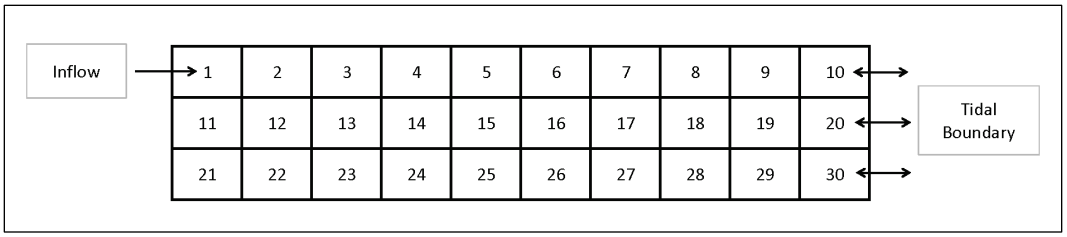

Each cell in the grid is assigned a unique number or index (Figure 2). Interfaces are numbered where flows pass between cells or where cells adjoin open boundaries. Faces adjacent to solid boundaries are not numbered. The grid is unstructured. That is, the cell index contains no information that indicates cell location in a 3D coordinate system. Neither is there a general relationship between the indices of adjacent cells or between cells and flow faces. A connectivity or *map* file is required that locates cells and faces relative to each other.

The unstructured grid of discrete volumes provides maximum flexibility in grid configuration. No restriction is placed on cell shape or number of flow faces per cell. In the complete ICM, the flows between cells usually come from an accompanying hydrodynamic model. The map file is constructed by software appended to the hydrodynamic model. For ICM-Lite, the user is anticipated to create the mapping for a relatively simple grid configuration. Flows are, likewise, anticipated to be entered by the user into a hydrodynamic file. These flows may be extracted from a hydrodynamic model or derived otherwise, for example, from stream gauges. The configuration of the map and hydrodynamic files will be described in the users' guide to be produced in the second study year.

Figure 2. The numbering system for cells, faces, and flows. The numbering scheme corresponds to the upper left cells in the grid shown in Figure 1.

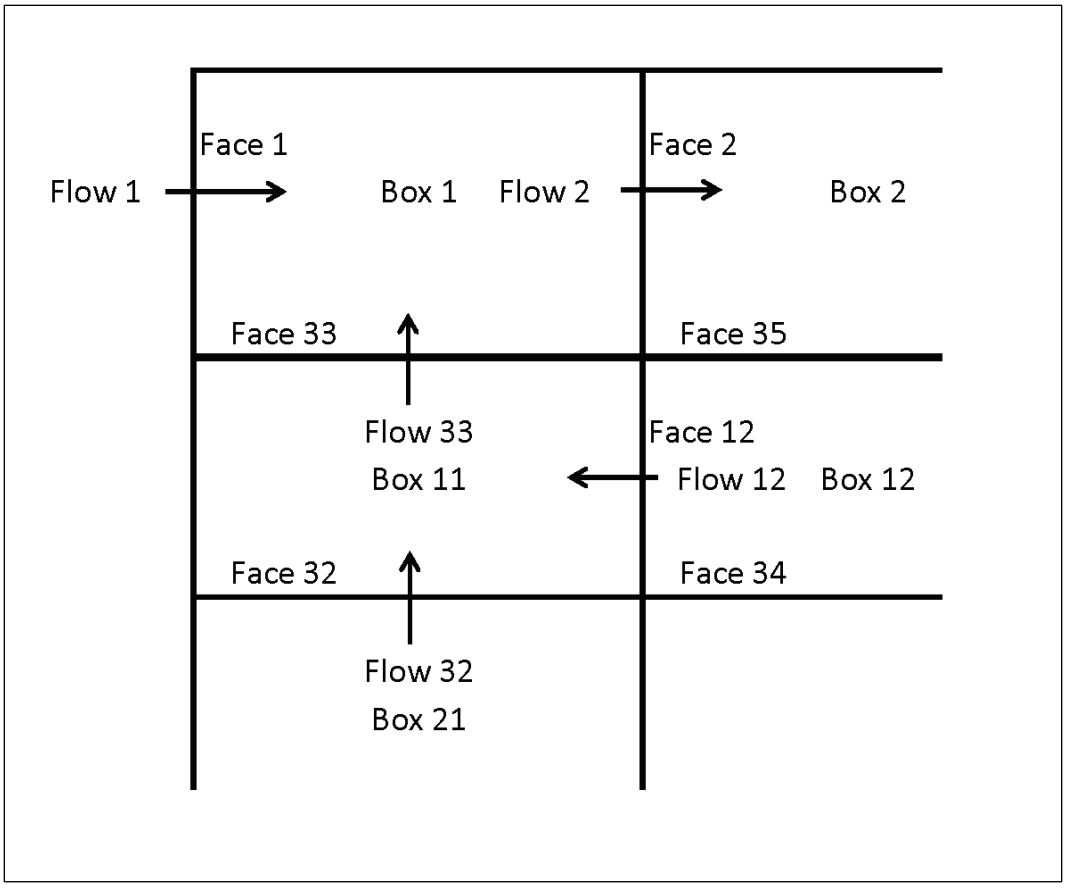

2.2 The conservation of mass equation

The foundation of ICM is the 3D mass conservation equation for a control volume. ICM solves, for each volume and for each state variable, the following equation:

$$\frac{\delta V_j \cdot C_j}{\delta t} = \sum_{k=1}^{n} Q_k \cdot C_k + \sum_{k=1}^{n} A_k \cdot D_k \cdot \frac{\delta C}{\delta x_k} + \sum S_j \quad (1)$$

in which:

V_j = volume of jth control volume (m^3)
C_j = concentration in jth control volume (g m^{-3})
Q_k = volumetric flow across flow face k of jth control volume (m^3 s^{-1})
C_k = concentration in flow across flow face k (g m^{-3})
A_k = area of flow face k (m^2)

D_k = diffusion coefficient at flow face k ($m^2\ s^{-1}$)
n = number of flow faces attached to jth control volume
S_j = external loads and kinetic sources and sinks in ith control volume ($g\ s^{-1}$)
t, x = temporal and spatial coordinates

2.3 Discretization of the mass conservation equation

Solution of the conservation-of-mass equation on a digital computer requires specification of parameter values and discretization of the continuous derivatives. Numerous formulae for evaluation and discretization exist. Formulae employed in ICM were selected based on computational efficiency and accuracy.

The conservation-of-mass equation is solved in two steps. In the first step, an intermediate value is computed. The intermediate value includes the effects of change in cell volume, longitudinal and lateral transport, and external loading. In the second step, the effects of vertical transport are computed.

2.3.1 Longitudinal and lateral advection

Solution to the conservation of mass equation in the longitudinal and lateral directions is via explicit time-stepping. That is:

$$C_j^* = \frac{V_j}{V_j^{t+\Delta t}} \cdot C_j + \frac{\Delta t}{V_j^{t+\Delta t}} \left[\sum_{k=1}^{nhf} Q_k \cdot C_k + \sum_{k=1}^{nhf} A_k \cdot D_k \cdot \frac{\delta C}{\delta x_k} + \sum S_j \right] \quad (2)$$

in which:

C_j^* = concentration in jth control volume after volume change, loading, longitudinal/lateral transport processes
$V_j^{t+\Delta t}$ = volume of jth control volume at time $t=\Delta t$
Δt = discrete time-step
nhf = number of longitudinal and lateral flow faces attached to jth control volume

Except where noted by $t+\Delta t$, all terms in Equation 2 are evaluated at time t.

Solution of Equation 2 requires evaluation of the concentrations flowing across cell faces, C_k. Two options are provided within ICM. The first is

backwards or upwind differencing. In upwind differencing, concentration in the flow across any face is taken as concentration in the cell upstream of the face (Figure 3). Upstream is defined relative to direction of the flow. Upstream has no relation to the cell coordinate system.

Figure 3. Derivation of *Ck* at cell faces for QUICKEST and UPWIND schemes.

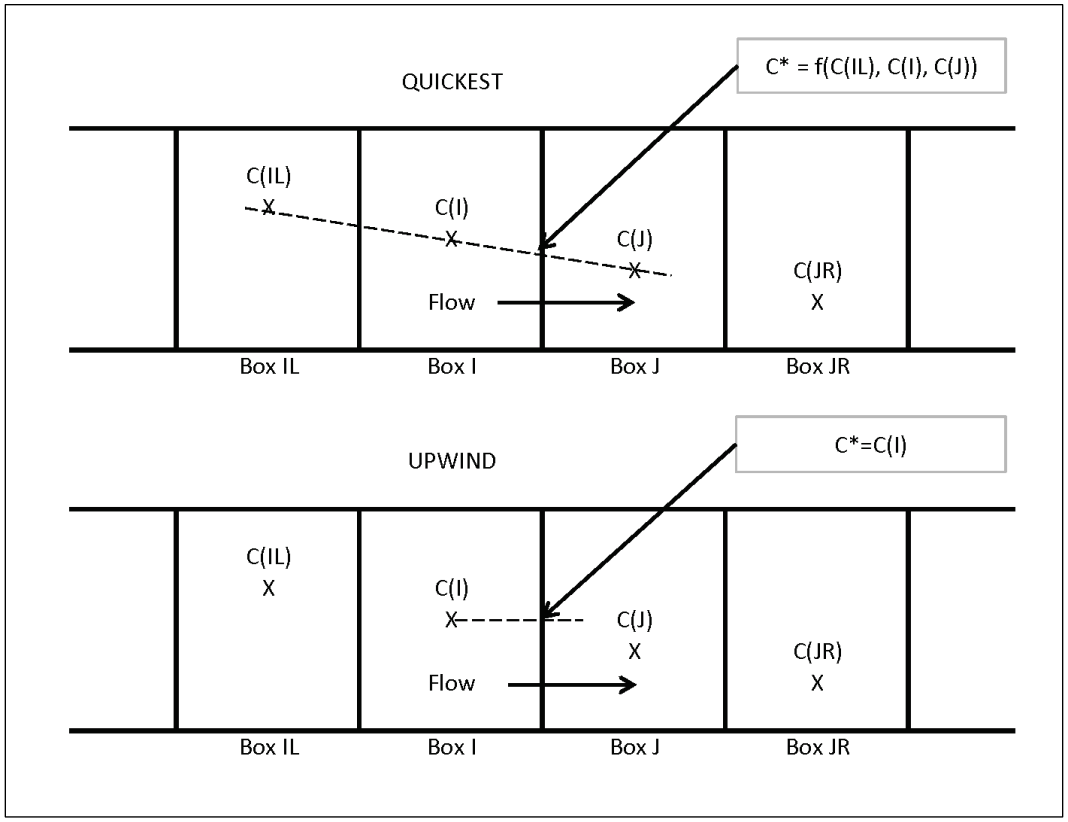

A second approximation to C_k fits a parabola to concentration in three adjacent cells (Figure 3). For uniform grid spacing,

$$C_k = \frac{1}{2}\left[C_i + C_j\right] - \frac{1}{8}\left[C_{il} + C_j - 2C_i\right] \tag{3}$$

The parabolic fit is part of a numerical scheme known as QUICKEST (Leonard 1979). While upwind differencing provides computational simplicity, the upwind method is less accurate and less stable than QUICKEST. The primary disadvantage of QUICKEST is that the method sometimes generates negative concentrations when advecting sharp concentration gradients. A second disadvantage is that QUICKEST cannot be implemented on highly irregular grids in which two adjacent upstream cells cannot be readily identified.

Detailed knowledge of the advective solution schemes is not necessary to execute the model. The upwind and QUICKEST approximations were reviewed to indicate the information required by the model to compute advective transport in the longitudinal and lateral directions. To compute advective transport in any cell, the model requires

- cell volume
- indices of longitudinal and lateral flow faces adjoining the cell
- indices of adjoining and next-most adjoining cells
- volumetric flow across the indexed flow faces
- length of indexed cells.

The required information is provided in the map, geometry, and hydrodynamics files. Formats of these files are provided in the users' guide.

2.3.2 Longitudinal and lateral dispersion

Computation of longitudinal and lateral dispersion requires discrete approximation of the continuous derivative in the dispersion term of Equation 2. The basic approximation is

$$\frac{\delta C}{\delta x_k} = \frac{C_j - C_i}{\Delta X} \tag{4}$$

in which:

Δx = distance between centers of two cells

A higher-order correction to the basic expression is computed when the QUICKEST scheme is employed.

2.3.3 Vertical transport

Solution to the conservation-of-mass equation in the longitudinal and lateral directions is by an explicit method. That is, all parameters in the discretized equation are evaluated at time t except the unknown C^*. The explicit method is suited for transport dominated by advection rather than diffusion or dispersion. In the vertical direction, diffusion is a significant or dominant component of transport. Solution of vertical transport by an explicit method requires a small time-step and consumes large amounts of computer time. In ICM, solution to vertical transport is by a partly or fully

implicit scheme that practically frees the computation from stability conditions imposed by vertical transport.

The mass-conservation equation in the vertical direction (Figure 4) can be expressed as

$$\frac{C_j^{t+\Delta t} - C_j^*}{\Delta t} = (1-\theta)\cdot\sum_{k=1}^{nvf}\frac{Q_k \cdot C_k}{V_k} + \theta\cdot\sum_{k=1}^{nvf}\frac{Q_k^{t+\Delta t}\cdot C_k^{t+\Delta t}}{V_k^{t+\Delta t}} + \sum_{k=1}^{nvf}\frac{A_k \cdot D_k}{V_k^{t+\Delta t}}\cdot\frac{\delta C^{t+\Delta t}}{\delta z} \quad (5)$$

in which:

θ = implicit weighting factor ($0 \le \theta \le 1$)
nvf = number of vertical faces
z = vertical coordinate.

The implicit weighting factor, θ, determines whether vertical advection is computed explicitly ($\theta = 0$), implicitly ($\theta = 1$), or is weighted between the two extremes ($0 < \theta < 1$). Computational stability is enhanced as θ --> 1, at the expense of increased numerical diffusion. The value $\theta = 0.75$ is recommended.

Since vertical velocities are usually much less than longitudinal velocities, the enhanced accuracy of the QUICKEST scheme is not necessary. Concentrations at cell interfaces, C_k and $C_k^{t+\Delta t}$, are computed by linear interpolation between concentrations at the centers of adjoining cells:

$$C_k = \frac{C_i \cdot \Delta z_i + C_j \cdot \Delta z_j}{\Delta z_i + \Delta z_j} \quad (6)$$

The spatial gradient in the diffusion term is evaluated by central difference evaluated at time-step $t+\Delta t$.

The solution scheme for vertical transport is an implicit scheme, which means that the equation for concentration in any cell at time $t+\Delta t$ (e.g., Equation 5) contains multiple unknowns. Computation of concentration in any one cell requires solution of a set of simultaneous equations for concentrations in a column of cells extending from water surface to

Figure 4. Definition of INFLOW, OUTFLOW, and TIDAL boundary conditions. *Cb* is a user-specified boundary concentration.

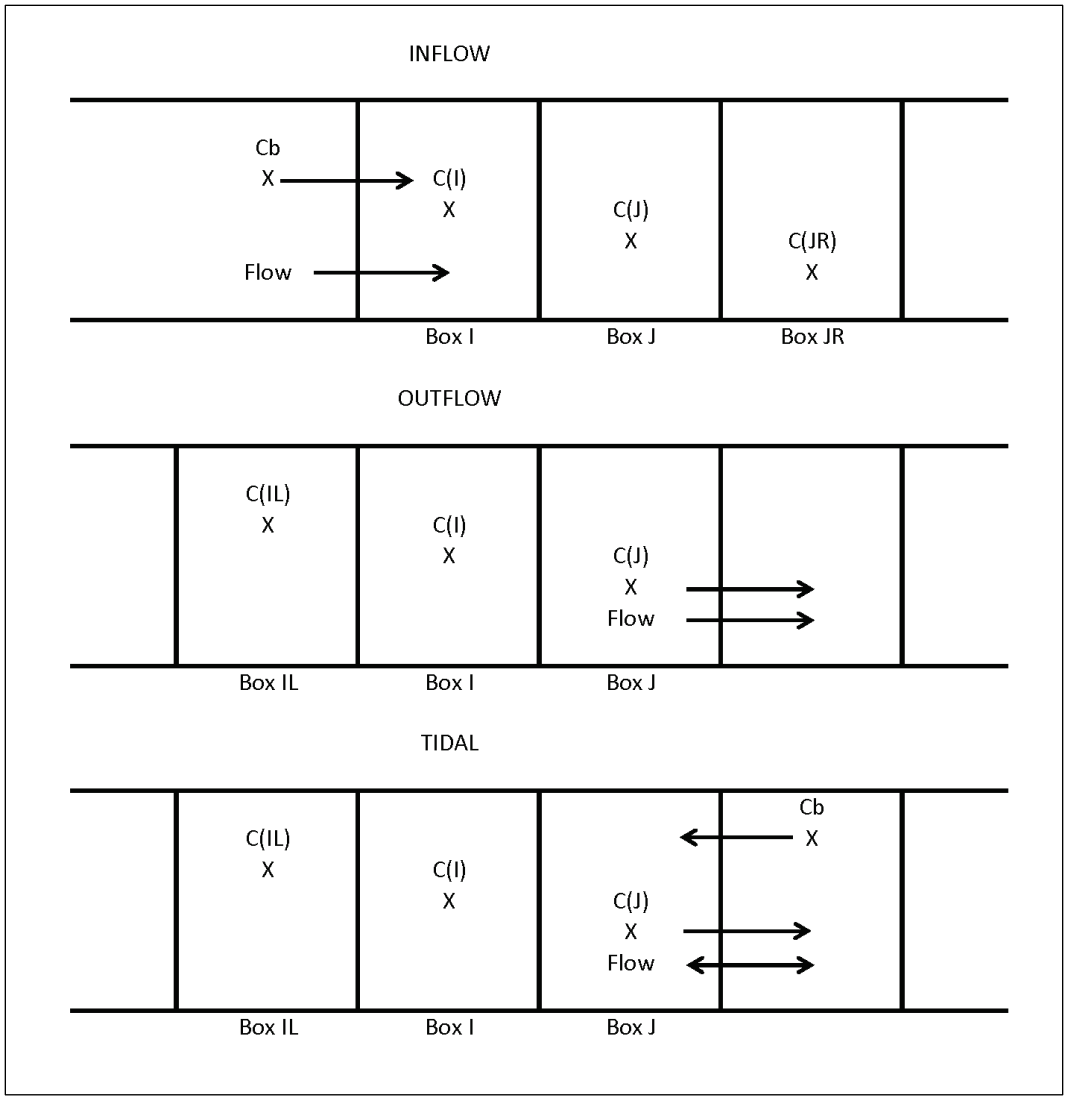

bottom. Details of the solution scheme are not necessary to operate the model. The user must provide, however, the following information required to compute vertical transport:

- indices of all cells in a column
- indices of vertical flow faces adjoining all cells in a column
- volumes of all cells in a column
- volumetric flow across the indexed flow faces
- diffusion coefficients at indexed flow faces
- length of indexed cells.

The required information is provided in the map, geometry, and hydrodynamics files. Formats of these files are provided in the users' guide (in preparation).

2.3.4 Summary of numerical solution scheme

The model solves the conservation-of-mass equation through a step-by-step procedure:

1. Evaluate internal sources and sinks. These include kinetics transformations and sediment-water fluxes. This step provides a partial computation of ΣS_j in Equation 1.
2. Add effects of external loads. This step completes computation of ΣS_j in Equation 1.
3. Specify longitudinal and lateral advection and diffusion at all interfaces. This step provides quantities required to solve Equation 2.
4. Compute concentration at time $t+\Delta t$ in all cells resulting from volume changes, kinetics, external loads, and longitudinal/lateral transport. This step is the solution to Equation 2. For 1D or 2D (longitudinal/lateral) systems, solution of the conservation-of-mass equation is complete at this point. For 2D (longitudinal/vertical) or 3D systems, the result is an intermediate solution prior to computation of vertical transport.
5. Compute vertical transport from surface to bottom. Computation is by columns. Each cell at the water surface represents the top of one column.

2.4 ICM time-step

Temporal integration of the conservation-of-mass equation (1) is accomplished in discrete time-steps Δt (Equations 2, 5). Integration in discrete steps provides an approximation to the continuous solution of the original differential equation. As Δt --> 0, the solution of the approximate equation converges on the solution of the continuous equation, although at great cost in computation time. As Δt --> ∞, computation time diminishes, but the solution of the discrete equation diverges from solution of the continuous equation. For sufficiently large Δt, the numerical solution may exhibit large oscillations or instabilities that produce computational failures. The occurrence of instabilities is prevalent in explicit rather than implicit solution schemes. Typical practice in numerical modeling is to select the largest time-step possible, to minimize computation time, while remaining in predefined stability limits.

The time-step employed is determined by an *autostepping* algorithm. The algorithm computes permissible time-step based on flow, dispersion, and cell dimension. As a consequence of autostepping, the time-step varies throughout a model run. The time-step is always near the maximum permissible time-step. Autostepping minimizes computation time while meeting stability requirements. For typical ICM applications, the time-step is on the order of minutes.

2.5 Boundary conditions

Boundary conditions must be specified at the flow faces along the edges of the grid. Through these faces, material is exchanged with the environment outside the model domain. Boundary flow faces are allowed only at the longitudinal and lateral limits of the grid. No flow is allowed through the surface and bottom. Cell faces at the water surface and bottom are not indexed, nor are cell faces indexed along longitudinal and lateral edges of the grid through which flow does not occur.

Treatment of open boundary conditions requires selection of the numerical scheme and specification of concentration in the environment beyond the grid. Three types of boundary conditions are defined: inflow boundaries, outflow boundaries, and tidal boundaries (Figure 4).

2.5.1 Inflow boundary conditions

Flow at inflow boundaries is unidirectional into the model domain. Typical inflow boundaries include flow at an estuarine fall line and river inflow at the head of a reservoir. The model employs upwind differencing at inflow boundaries. Upwind differencing occurs whether or not the QUICKEST scheme is specified for advection within the interior of the grid. Upwind differencing ensures that the concentration of flow entering the domain is the specified boundary concentration. If QUICKEST were employed at an inflow boundary, the three-point weighting scheme would compute an influence of concentration within the system on concentration entering the system. Dispersion is set to zero at inflow boundaries to ensure that the mass entering the system is determined exactly as the product of flow and concentration.

2.5.2 Outflow boundary conditions

Flow at outflow boundaries is unidirectional out of the model domain. Typical outflow boundaries include flow over a spillway and flow at the downstream end of a modeled river reach. The model employs upwind differencing at outflow boundaries. Upwind differencing occurs whether or not the QUICKEST scheme is specified for advection within the interior of the grid. Upwind differencing ensures that the concentration of flow leaving the domain is determined solely by conditions within the domain. If QUICKEST were employed at an outflow boundary, the three-point weighting scheme would compute an influence of concentration outside the system on concentration leaving the system. This situation is clearly impossible at a spillway, for example. Dispersion is set to zero at outflow boundaries based on the same reasoning. Material leaving the system cannot mix back into the system.

2.5.3 Tidal boundaries

The typical tidal boundary is situated at the mouth of an estuary or lagoon. Flow at tidal boundaries is bidirectional, depending on the phase of the tide. Flow is into the system on the flood tide and out of the system on the ebb. Material is free to mix in both directions across the interface. The model employs upwind or QUICKEST at tidal boundaries, depending on the scheme specified for the interior of the system. Dispersion is calculated at tidal boundaries.

3 Kinetics in the Water Column

The *Lite* version of ICM incorporates 11 state variables in the water column:

- temperature
- salinity
- fixed suspended solids
- phytoplankton (as carbon)
- organic carbon
- ammonium
- nitrate
- organic nitrogen
- phosphate
- organic phosphorus
- dissolved oxygen.

An additional user-defined variable can be implemented to provide basic representation of a substance, such as bacteria or contaminant, not in the standard model suite. Additional quantities can be derived from the state variable suite. Diffuse light attenuation is one important derived variable which is calculated based on computed organic and inorganic particulate matter.

The fate and transport of all model state variables are computed based on the mass conservation equation (Equation 1) presented in the preceding chapter. For notational simplicity, the transport terms are dropped from the equation when describing the kinetics formulations which contribute to the ΣS_j.

3.1 Temperature

Computation of temperature employs a conservation of internal energy equation that is analogous to the conservation of mass equation. For practical purposes, the internal energy equation can be written as a conservation of temperature equation. The only source or sink of temperature considered is exchange with the atmosphere. Atmospheric exchange is considered proportional to the temperature difference

between the water surface and a theoretical equilibrium temperature (Edinger et al. 1974):

$$\frac{\delta}{\delta t}T = \frac{KT}{\rho \cdot Cp \cdot H} \cdot (Te - T) \tag{7}$$

in which:

T = water temperature (°C)
Te = equilibrium temperature (°C)
KT = heat exchange coefficient (watt m^{-2} $°C^{-1}$)
Cp = specific heat of water (4200 watt s kg^{-1} $°C^{-1}$)
ρ = density of water (1000 kg m^{-3})
H = depth of water column or surface cell (m).

3.2 Salinity

Salinity is modeled by the conservation of mass equation with no internal sources or sinks

3.3 Fixed solids

Fixed solids comprise the inorganic particles suspended in the water column. (Total Suspended Solids is a derived quantity based on computed fixed solids and organic matter). The only internal source or sink of fixed solids is settling:

$$\frac{\delta}{\delta t}FS = -Ws \cdot \frac{\delta}{\delta z}FS \tag{8}$$

in which:

FS = fixed solids concentration (g m^{-3})
Ws = fixed solids settling rate (m d^{-1})
z = vertical coordinate.

3.4 Light attenuation

Irradiance decreases exponentially as a function of depth below the water surface:

$$I(z) = Io \cdot e^{-Ke \cdot z} \tag{9}$$

in which:

$I(z)$ = irradiance at depth z (E m^{-2} d^{-1})
Io = irradiance at water surface (E m^{-2} d^{-1})
Ke = diffuse light attenuation coefficient (m^{-1}).

The diffuse light attenuation coefficient is computed by a partial attenuation model based on computed suspended solids:

$$Ke = a1 + a2 \cdot FS + a3 \cdot VSS \tag{10}$$

in which:

Ke = coefficient of diffuse light attenuation (m^{-1})
$a1$ = background attenuation (m^{-1})
$a2$ = attenuation by inorganic suspended solids (m^2 g^{-1})
$a3$ = attenuation by organic suspended solids (m^2 g^{-1})
FS = inorganic (fixed) suspended solids concentration (g m^{-3})
VSS = organic (volatile) suspended solids concentration (g m^{-3}).

The empirical coefficients a1–a3 are provided by the user. *VSS* is based on computed organic matter concentration. The units of irradiance and of *Ke* are determined by requirements of the phytoplankton model. Often, water quality or habitat criteria are based on turbidity, which is a measure of optical scattering. Turbidity is a derived quantity which can also be represented as an empirical function of suspended solids concentration. The option to compute turbidity will be provided in the GUI.

3.5 Phytoplankton

Algal sources and sinks in the conservation equation include production, respiration, predation, and settling. These are expressed:

$$\frac{\delta}{\delta t} B = \left[G - R - Wa \cdot \frac{\delta}{\delta z} \right] \cdot B - PR \tag{11}$$

in which:

B = algal biomass, expressed as carbon (g C m^{-3})
G = growth (d^{-1})
R = respiration (d^{-1})
Wa = algal settling velocity (m d^{-1})
PR = predation (g C m^{-3} d^{-1})
z = vertical coordinate.

3.5.1 Production

Production by phytoplankton is determined by the intensity of light, by the availability of nutrients, and by the ambient temperature.

3.5.2 Light

The influence of light on phytoplankton production is represented by a chlorophyll-specific production equation (Jassby and Platt 1976):

$$P^B = P^B m \cdot \frac{I}{\sqrt{I^2 + Ik^2}} \tag{12}$$

in which:

P^B = photosynthetic rate (g C g^{-1} Chl d^{-1})
$P^B m$ = maximum photosynthetic rate (g C g^{-1} Chl d^{-1})
I = irradiance (E m^{-2} d^{-1}).

Parameter Ik is defined as the irradiance at which the initial slope of the production vs. irradiance relationship (Figure 5) intersects the value of $P^B m$:

$$Ik = \frac{P^B m}{\alpha} \tag{13}$$

in which:

α = initial slope of production vs. irradiance relationship (g C g^{-1} Chl (E m^{-2})$^{-1}$)

Figure 5. The production vs. irradiance curve. When I << Ik, production depends on available light. When I >> Ik, production approaches a maximum independent of available light.

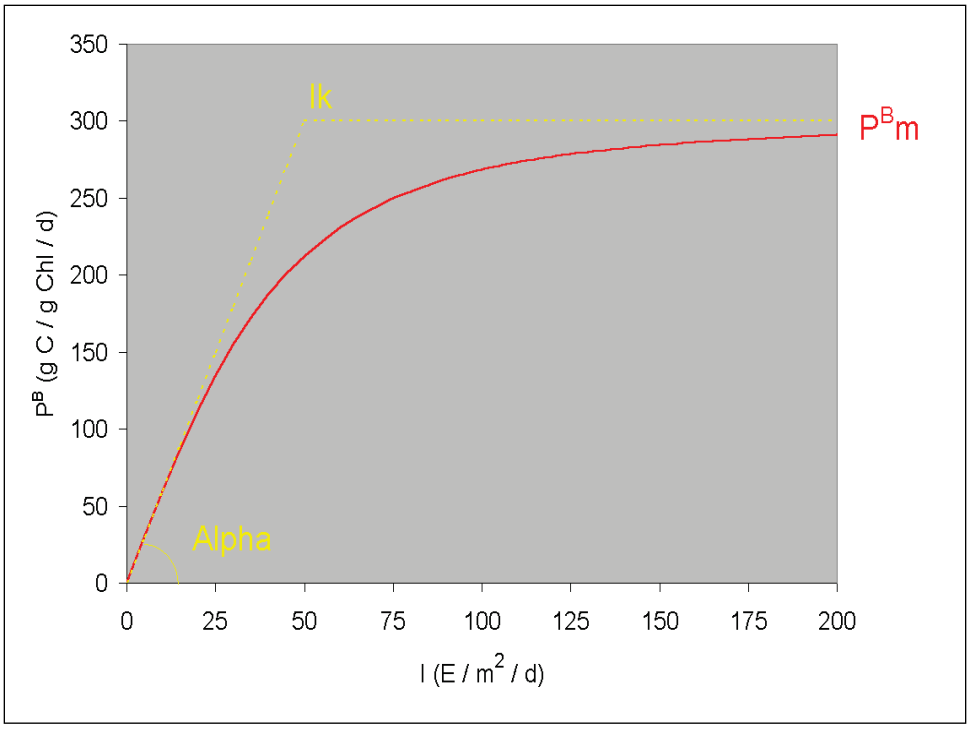

The chlorophyll-specific production rate, P^B, is readily converted to carbon specific growth rate, for use in Equation 11, through division by the carbon-to-chlorophyll ratio:

$$G = \frac{P^B}{CChl} \tag{14}$$

in which:

$CChl$ = carbon-to-chlorophyll ratio (g C g^{-1} chlorophyll a).

3.5.3 Nutrients

Carbon, nitrogen, and phosphorus are the primary nutrients required for algal growth. Diatoms require silica, as well. Inorganic carbon and silica are usually available in excess and are not considered in the model. The effects of the remaining nutrients on growth are described by the formulation commonly referred to as “Monod kinetics” (Figure 6; Monod 1949):

$$f(N) = \frac{D}{KHd + D} \tag{15}$$

in which:

$f(N)$ = nutrient limitation on algal production ($0 \leq f(N) \leq 1$)
D = concentration of dissolved nutrient (g m^{-3})
KHd = half-saturation constant for nutrient uptake (g m^{-3}).

Figure 6. Monod formulation for nutrient-limited growth. N/KH is the ratio of available nutrient concentration to the half-saturation concentration for nutrient uptake.

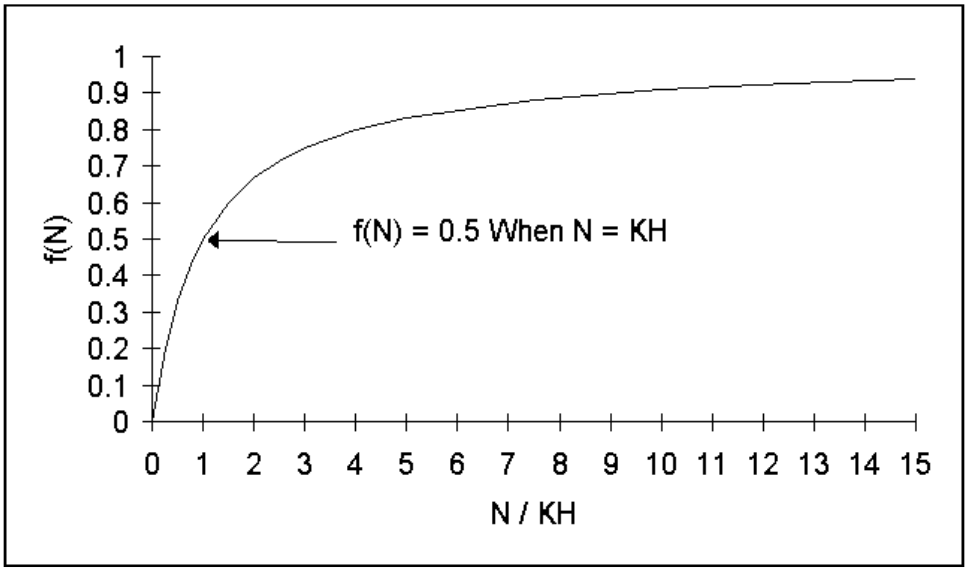

3.5.4 Temperature

Algal production increases as a function of temperature until an optimum temperature or temperature range is reached. Above the optimum, production declines until a temperature lethal to the organisms is attained. Numerous functional representations of temperature effects are available. Inspection of growth vs. temperature data indicates a function similar to a Gaussian probability curve (Figure 7) provides a good fit to observations:

$$f(T) = e^{-KTg1\cdot(T-Topt)^2} \; when \; T \leq Topt \tag{16}$$

$$f(T) = e^{-KTg2\cdot(Topt-T)^2} \; when \; T > Topt \tag{17}$$

in which:

T = temperature (°C)
$Topt$ = optimal temperature for algal growth (°C)
$KTg1$ = effect of temperature below $Topt$ on growth ($°C^{-2}$)
$KTg2$ = effect of temperature above $Topt$ on growth ($°C^{-2}$).

Figure 7. Dependence of algal production on temperature.

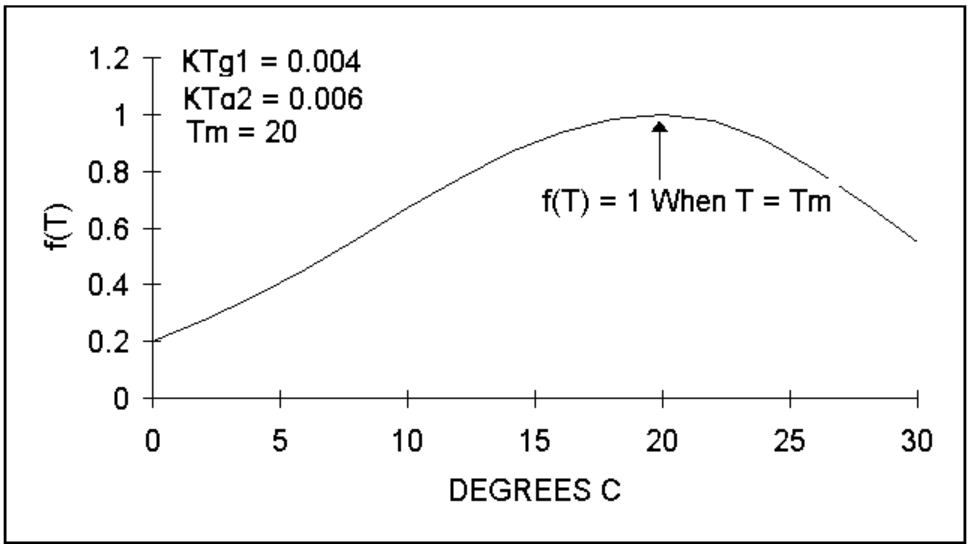

3.5.5 Combining the effects of light, nutrients, and temperature

A production vs. irradiance relationship (Equation 12) is constructed for each model cell at each time-step. First, the maximum photosynthetic rate under ambient temperature and nutrient concentrations is determined:

$$P^B m\left(N,T\right) = P^B m \cdot f(T) \cdot f(N) \tag{18}$$

in which:

$P^B m(N,T)$ = maximum photosynthetic rate under ambient temperature and nutrient concentrations (g C g^{-1} Chl d^{-1})

The most limiting nutrient is employed in determining the nutrient limitation, $f(N)$. Next, parameter Ik is derived from Equation 13. Finally, the production vs. irradiance relationship is constructed using $P^B m(N,T)$ and Ik. The production vs. irradiance relationship allows the calculation of growth rate, G, at any depth and level of irradiance via Equation 14.

3.5.6 Respiration

Two forms of respiration are considered in the model: photo-respiration and basal metabolism. Photo-respiration represents the energy expended by carbon fixation and is a fixed fraction of production. In the event of no production (e.g., at night), photo-respiration is zero. Basal metabolism is a continuous energy expenditure to maintain basic life processes. In the model, metabolism is considered to be an exponentially increasing function of temperature (Figure 8). Total respiration is represented:

$$R = Presp \cdot G + BM \cdot e^{KTb \cdot (T - Tr)} \tag{19}$$

in which:

$Presp$ = photo-respiration ($0 \leq Presp \leq 1$)
BM = metabolic rate at reference temperature Tr (d^{-1})
KTb = effect of temperature on metabolism ($^oC^{-1}$)
Tr = reference temperature for metabolism (^oC).

Figure 8. Exponential temperature relationship employed for algal metabolism and other processes.

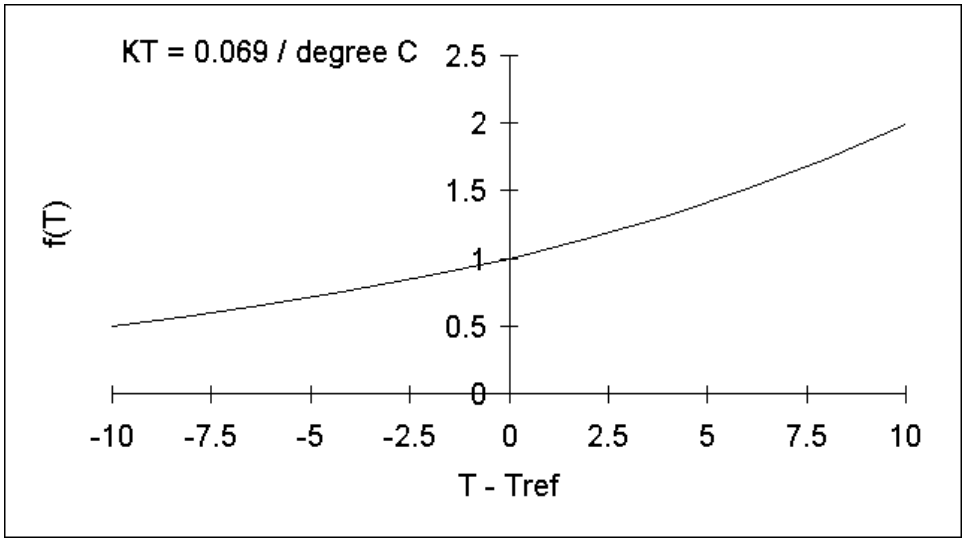

3.5.7 Predation

Predation is modeled by assuming predators clear a specific volume of water per unit biomass:

$$PR = F \cdot B \cdot M \tag{20}$$

in which:

F = filtration rate ($m^3\ g^{-1}$ predator C d^{-1})
M = planktivore biomass (g C m^{-3}).

Detailed specification of the spatial and temporal distribution of the predator population is impossible. One approach is to assume predator biomass is proportional to algal biomass, $M = \gamma B$, in which case Equation 20 can be rewritten:

$$PR = \gamma \cdot F \cdot B^2 \tag{21}$$

Equation 21 results in a quadratic predation term; predation rate is proportional to the algal biomass squared. This formulation is recommended by Cerco and Noel (2004) based on comparisons of computed and observed algal biomass and production in Chesapeake Bay. To provide maximum model flexibility, however, the exponent on algal biomass is a user-specified variable. The predation term as expressed in the model code follows:

$$PR = BPR \cdot B^{PRP} \tag{22}$$

in which:

BPR = basic predation rate ($m^3\ g^{-1}$ C d^{-1})
PRP = predation power.

The value $PRP = 2$ results in the recommended formulation. The value $PRP = 1$ results in a first-order loss term which is in common usage. The units of BPR vary, depending on the value of PRP. The units specified above are for $PRP = 2$.

3.5.8 Accounting for algal nitrogen

Model nitrogen state variables include ammonium, nitrate, and organic nitrogen. The amount of nitrogen incorporated in algal biomass is quantified through a stoichiometric ratio. Thus, total nitrogen in the model is expressed:

$$TotN = NH_4 + NO_3 + Anc \cdot B + OrgN \tag{23}$$

in which:

$TotN$ = total nitrogen (g N m^{-3})
NH_4 = ammonium (g N m^{-3})
NO_3 = nitrate (g N m^{-3})
Anc = algal nitrogen-to-carbon ratio (g N g^{-1} C)
$OrgN$ = organic nitrogen (g N m^{-3}).

Algae take up ammonium and nitrate during production and release ammonium and organic nitrogen through respiration. The fate of nitrogen released by respiration is determined by empirical distribution coefficients. The fate of algal nitrogen recycled by predation is determined by a second set of distribution parameters.

3.5.9 Algal nitrogen preference

Algae can utilize ammonium and nitrate for production. Trace concentrations of ammonium inhibit nitrate uptake so that, in the presence of multiple nitrogenous nutrients, ammonium is utilized first. The *preference* of algae for ammonium is expressed by a modification of an empirical function presented by Thomann and Fitzpatrick (1982):

$$PN = NH_4 \cdot \frac{NO_3}{(KHNH_4 + NH_4) \cdot (KHNH_4 + NO_{3)}} + NH_4 \cdot \frac{KHNH_4}{(NH_4 + NO_3) \cdot (KHNH_4 + NO_{3)}} \quad (24)$$

in which:

PN = algal preference for ammonium uptake ($0 \leq PN \leq 1$)
$KHNH_4$ = half saturation concentration for algal ammonium uptake (g N m^{-3}).

The preference function has two limiting values (Figure 9). When nitrate is absent, the preference for ammonium is unity. When ammonium is absent, the preference is zero. In the presence of ammonium and nitrate, the preference depends on the abundance of both forms relative to the half-saturation constant for nitrogen uptake. When both ammonium and nitrate are abundant, the preference for ammonium approaches unity. When ammonium is scarce but nitrate is abundant, the preference decreases in magnitude, and a significant fraction of algal nitrogen requirement comes from nitrate.

Figure 9. Algal ammonium preference. The preference depends on the abudance of ammonium and nitrate relative to the half-saturation concentration for algal ammonium uptake, $KHNH_4$.

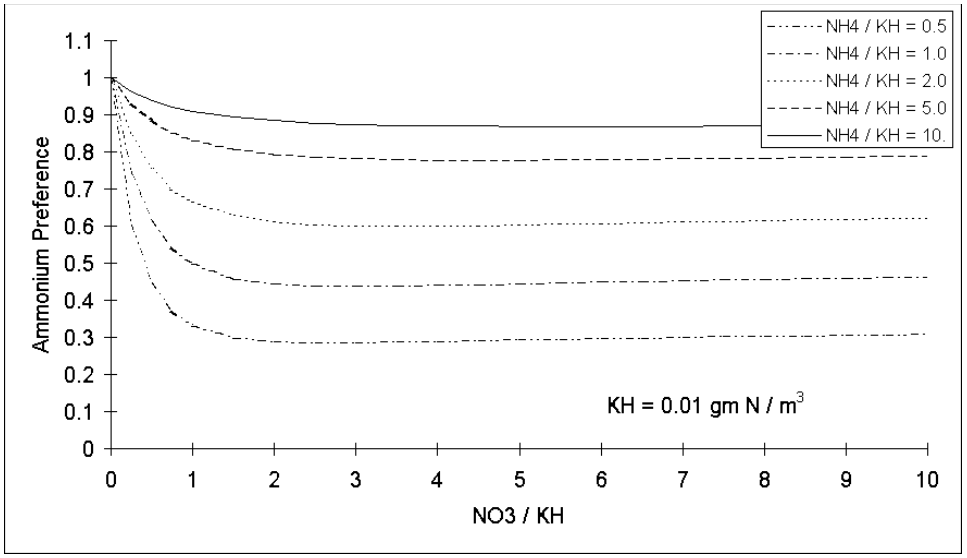

3.5.10 Accounting for algal phosphorus

As with nitrogen, the amount of phosphorus incorporated in algal biomass is quantified through a stoichiometric ratio. Thus, total phosphorus in the model is expressed:

$$TotP = PO_4 + Apc \cdot B + OrgP \tag{25}$$

in which:

$TotP$ = total phosphorus (g P m^{-3})
PO_4 = dissolved phosphate (g P m^{-3})
Apc = algal phosphorus-to-carbon ratio (g P g^{-1} C)
$OrgP$ = organic phosphorus (g P m^{-3}).

Algae take up phosphate during production and release phosphate and organic phosphorus through respiration. The fate of phosphorus released by respiration is determined by empirical distribution coefficients. The fate of algal phosphorus recycled by predation is determined by a second set of distribution parameters.

3.5.11 Effect of algae on dissolved oxygen

Algae produce oxygen during photosynthesis and consume oxygen through respiration. The quantity produced depends on the form of

nitrogen utilized for growth. When ammonium is the nitrogen source, one mole oxygen is produced per mole carbon dioxide fixed. When nitrate is the nitrogen source, 1.3 moles oxygen are produced per mole carbon dioxide fixed.

In addition to algal respiration, the model allows for a portion of algal biomass lost to predation to be represented as oxygen consumption. This consumption represents respiration by predators. Oxygen consumption is limited to the amount available. In the event dissolved oxygen (DO) concentration is insufficient to supply the respiratory demand, a portion of respiration is instead allocated to release of organic carbon. The equation that describes the effect of algae on dissolved oxygen in the model follows:

$$\frac{\delta}{\delta t} DO = \left[(1.3 - 0.3 \cdot PN) \cdot G - (1 - FC) \cdot R \right] \cdot AOCR \cdot B - FDOP \cdot (1 - FC) \cdot AOCR \cdot PR \quad (26)$$

in which:

FC = fraction of oxygen consumption recycled as organic carbon due to low DO concentration ($0 \leq FC \leq 1$)

$AOCR$ = dissolved oxygen-to-carbon ratio in respiration (2.67 g O_2 g^{-1} C)

$FDOP$ = fraction of predation expressed as oxygen consumption ($0 < FDOP < 1$).

The quantity ($1.3 - 0.3 \cdot PN$) is the photosynthesis ratio and expresses the molar quantity of oxygen produced per mole carbon fixed. The photosynthesis ratio approaches unity as the algal preference for ammonium approaches unity. The fraction of oxygen consumption recycled as organic carbon is represented:

$$FC = \frac{KHr}{KHr + DO} \quad (27)$$

in which:

KHr = dissolved oxygen concentration at which oxygen consumption is halved (g DO m^{-3}).

3.6 Organic carbon

Organic carbon undergoes numerous transformations in the water column. The model carbon cycle (Figure 10) consists of the following elements:

- phytoplankton production and excretion
- predation on phytoplankton
- heterotrophic respiration
- settling.

Figure 10. The model carbon cycle. Phytoplankton and organic carbon are model state variables.

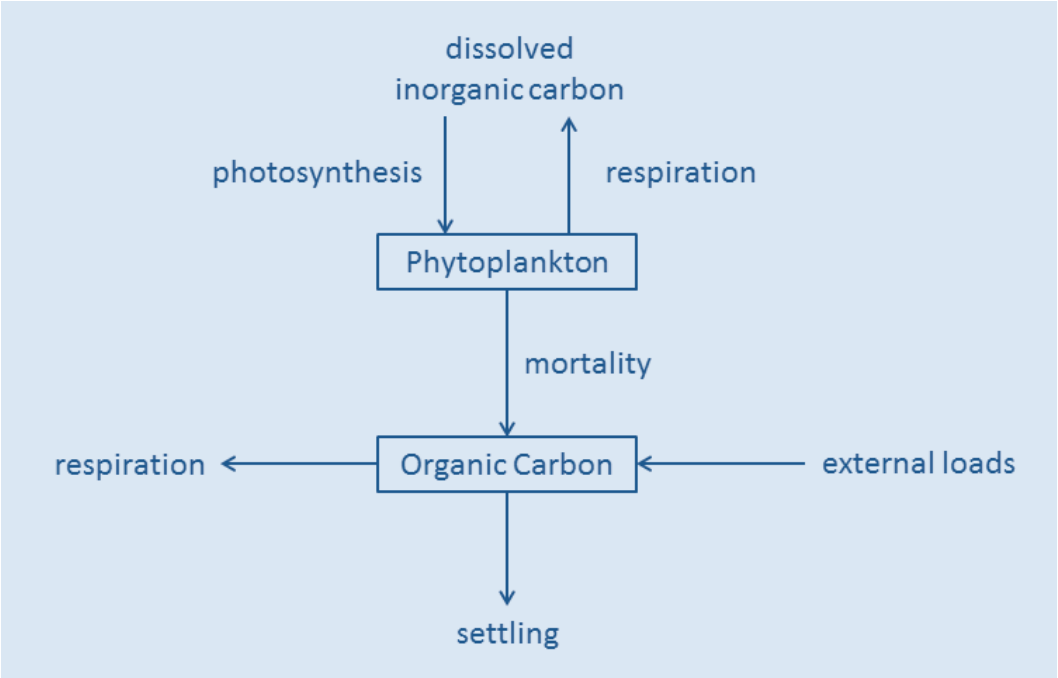

Algal production is frequently the primary carbon source although carbon also enters the system through external loading. Predation on algae by zooplankton and other organisms releases organic carbon to the water column. Organic carbon is respired at a first-order rate to inorganic carbon. A portion of the organic carbon which does not undergo respiration settles to the bottom sediments.

Organic carbon respiration is represented as a first-order process in which the reaction rate is proportional to concentration of the reactant. The reaction is restricted at low DO concentrations. An exponential function

(Figure 8) relates respiration to temperature. The complete representation of organic carbon sources and sinks in the model system follows:

$$\frac{\delta}{\delta t} OrgC = FC \cdot \left(R \cdot B + FDOP \cdot PR\right) + \left(1 - FDOP\right) \cdot PR - \frac{DO}{KHr + DO} \cdot Korgc \cdot OrgC - W_{op} \cdot \frac{\delta}{\delta z} OrgC \quad (28)$$

in which:

$OrgC$ = organic carbon (g m^{-3})
FC = fraction of algal and predator respiration released as $OrgC$ due to low DO concentration ($0 < FC < 1$)
R = algal respiration rate (d^{-1})
B = algal biomass (g m^{-3})
$FDOP$ = fraction of predation expressed as oxygen consumption ($0 < FDOP < 1$)
PR = predation on algae (g C m^{-3} d^{-1})
KHr = dissolved oxygen concentration at which respiration of organic carbon is halved (g DO m^{-3})
$Korgc$ = respiration rate of $OrgC$ (d^{-1})
Wop = settling rate for organic matter (m d^{-1})
z = vertical coordinate.

Predation contributes to $OrgC$ through two terms. The first represents the fraction of predation intended for oxygen consumption, but for which, the dissolved oxygen supply is insufficient. The second term is the fraction routed directly to $OrgC$ under all conditions.

3.7 Nitrogen

The model nitrogen cycle (Figure 11) includes the following processes:

- algal production and metabolism
- predation
- mineralization of organic nitrogen
- settling
- nitrification.

Figure 11. The model nitrogen cycle. Nitrate, ammonium, organic nitrogen and phytoplankton are model state variables.

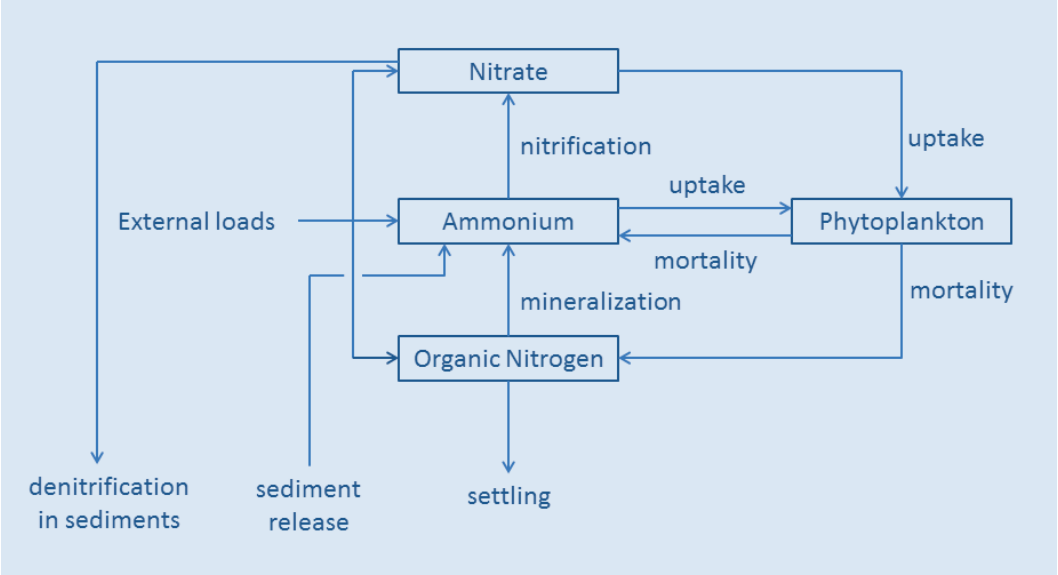

External loads are the ultimate source of nitrogen to the system. Available nitrogen (ammonium and nitrate) is incorporated by algae during growth and released as ammonium and organic nitrogen through respiration and predation. A portion of the organic nitrogen mineralizes to ammonium. An additional portion settles to the sediments. In an oxygenated water column, a fraction of the ammonium is subsequently oxidized to nitrate through the nitrification process. Organic nitrogen that settles to the sediments is mineralized and recycled to the water column, primarily as ammonium. Nitrate moves in both directions across the sediment-water interface, depending on relative concentrations in the water column and sediment interstices.

3.7.1 Nitrification

Nitrification is a process mediated by specialized groups of autotrophic bacteria that obtain energy through the oxidation of ammonium to nitrite and oxidation of nitrite to nitrate. A simplified expression for complete nitrification (Tchobanoglous and Schroeder 1987) follows:

$$NH_4^+ + 2O_2 \overset{yields}{\rightarrow} NO_3^- + H_2O + 2H^+ \quad (29)$$

The simplified stoichiometry indicates that two moles of oxygen are required to nitrify one mole of ammonium into nitrate. The simplified equation is not strictly true, however. Cell synthesis by nitrifying bacteria

is accomplished by the fixation of carbon dioxide so that less than two moles of oxygen are consumed per mole ammonium utilized (Wezernak and Gannon 1968).

The kinetics of complete nitrification are modeled as a function of available ammonium, dissolved oxygen, and temperature:

$$NT = \frac{DO}{KHont + DO} \cdot \frac{NH_4}{KHnnt + NH_4} \cdot f(T) \cdot NTm \tag{30}$$

in which:

NT = nitrification rate (g N m^{-3} d^{-1})
$KHont$ = half-saturation constant of dissolved oxygen required for nitrification (g O_2 m^{-3})
$KHnnt$ = half-saturation constant of NH_4 required for nitrification (g N m^{-3})
NTm = maximum nitrification rate at optimal temperature (g N m^{-3} d^{-1}).

The kinetics formulation (Figure 12) incorporates the products of two Monod-like functions. The first function diminishes nitrification at low dissolved oxygen concentration. The second function expresses the influence of ammonium concentration on nitrification. When ammonium concentration is low, relative to *KHnnt*, nitrification is proportional to ammonium concentration. For $NH4 << KHnnt$, the reaction is approximately first-order. (The first-order decay constant $\approx NTm/KHnnt$.) When ammonium concentration is large, relative to *KHnnt*, nitrification approaches a maximum rate. This formulation is based on a concept proposed by Tuffey et al. (1974). Nitrifying bacteria adhere to benthic or suspended sediments. When ammonium is scarce, vacant surfaces suitable for nitrifying bacteria exist. As ammonium concentration increases, bacterial biomass increases, vacant surfaces are occupied, and the rate of nitrification increases. The bacterial population attains maximum density when all surfaces suitable for bacteria are occupied. At this point, nitrification proceeds at a maximum rate independent of additional increase in ammonium concentration.

Figure 12. Effect of dissolved oxygen and ammonium concentrations on nitrification rate. When ammonium is abundant, NH_4 >> KHnt, nitrification rate, NT, approaches a maximum value. As dissolved oxygen diminishes, DO << KHnt, nitrification rate approaches zero.

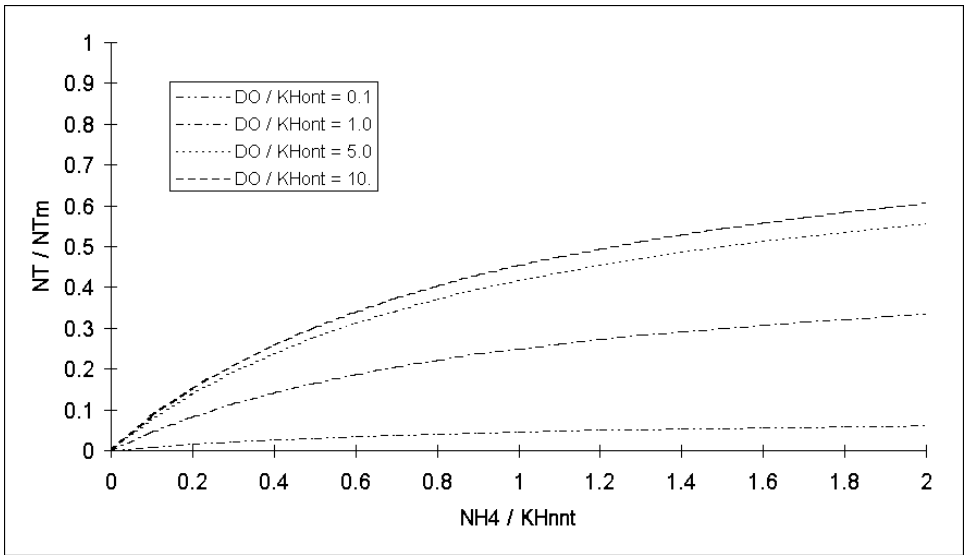

The optimal temperature for nitrification may be less than peak temperatures that occur in surface waters. To allow for a decrease in nitrification at superoptimal temperature, the effect of temperature on nitrification is modeled in the Gaussian form of Equations 16 and 17.

3.7.2 Nitrogen mass balance equations

The mass-balance equations for nitrogen state variables are written by summing all previouslydescribed sources and sinks:

3.7.2.1 Ammonium

$$\frac{\delta}{\delta t} NH_4 = Anc \cdot \left[\left(R \cdot FNI - PN \cdot G \right) \cdot B + PR \cdot FNIP \right] + Korgn \cdot OrgN - NT \quad (31)$$

in which:

Anc = algal nitrogen-to-carbon ratio (g N g^{-1} C)
R = algal respiration rate (d^{-1})
FNI = fraction of algal metabolism released as $NH4$ ($0 \leq FNI \leq 1$)
PN = algal ammonium preference ($0 \leq PN \leq 1$)

G = algal growth rate (d^{-1})
B = algal biomass ($g\ m^{-3}$)
PR = predation on algae ($g\ C\ m^{-3}\ d^{-1}$)
$FNIP$ = fraction of predation released as $NH4$ ($0 \leq FNIP \leq 1$)
$Korgn$ = organic nitrogen mineralization rate (d^{-1})
$OrgN$ = organic nitrogen ($g\ m^{-3}$).

3.7.2.2 Nitrate

$$\frac{\partial}{\partial t} NO_3 = -Anc \cdot (1 - PN) \cdot P \cdot B + NT \tag{32}$$

in which:

$NO3$ = nitrate concentration ($g\ m^{-3}$).

3.7.2.3 Organic Nitrogen

$$\frac{\delta}{\delta t} OrgN = Anc \cdot [R \cdot B \cdot (1 - FNI) + PR \cdot (1 - FNIP)] - Korgn \cdot OrgN - Wop \cdot \frac{\delta}{\delta z} OrgN \tag{33}$$

in which:

Wop = settling rate for organic matter ($m\ d^{-1}$)
z = vertical coordinate.

3.8 Phosphorus

The model phosphorus cycle (Figure 13) includes the following processes:

- algal uptake and excretion
- predation
- mineralization of organic phosphorus
- settling.

Figure 13. The model phosphorus cycle. Phosphate, organic phosphorus, and phytoplankton are model state variables.

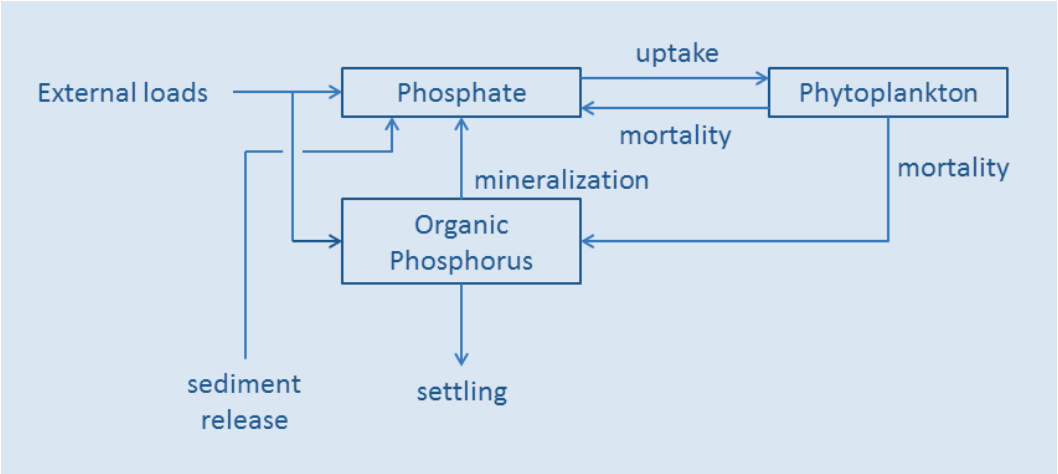

External loads are the ultimate source of phosphorus to the system. Dissolved phosphate is incorporated by algae during growth and released, along with organic phosphorus, through respiration and predation. A portion of the organic phosphorus is mineralized to phosphate. A second portion settles to the sediments. Within the sediments, organic phosphorus is mineralized and recycled to the water column as dissolved phosphate.

3.8.1 Phosphate

The mass balance equation for phosphate, including all processes, is

$$\frac{\delta}{\delta t} PO_4 = Korgp \cdot OrgP - Apc \cdot G \cdot B + Apc \cdot \left[FPI \cdot R \cdot B + FPIP \cdot PR \right] \quad (34)$$

in which:

$PO4$ = phosphate (g m^{-3})
$Korgp$ = organic phosphorus mineralization rate (d^{-1})
$OrgP$ = organic phosphorus (g m^{-3})
Apc = algal phosphorus-to-carbon ratio (g P g^{-1} C)
G = algal growth rate (d^{-1})
B = algal biomass (g m^{-3})
FPI = fraction of algal metabolism released as phosphate ($0 \le FPI \le 1$)
R = algal respiration rate (d^{-1})
$FPIP$ = fraction of predation released as phosphate ($0 \le FPIP \le 1$)

PR = predation on algae (g C m^{-3} d^{-1}).

3.8.2 Organic phosphorus

The mass balance equation for organic phosphorus, including all processes, is

$$\frac{\delta}{\delta t}OrgP = Apc \cdot \left[R \cdot B \cdot (1 - FPI) + PR \cdot (1 - FPIP)\right] - Korgp \cdot OrgP - Wop \cdot \frac{\delta}{\delta z}OrgP \quad (35)$$

in which:

Wop = settling rate for organic matter (m d^{-1})
z = vertical coordinate.

3.9 Dissolved oxygen

Sources and sinks of dissolved oxygen in the water column (Figure 14) include

- algal photosynthesis
- atmospheric reaeration
- algal respiration
- heterotrophic respiration
- nitrification.

Figure 14. The model dissolved oxygen cycle. Phytoplankton, dissolved oxygen, ammonium, and organic carbon are model state variables.

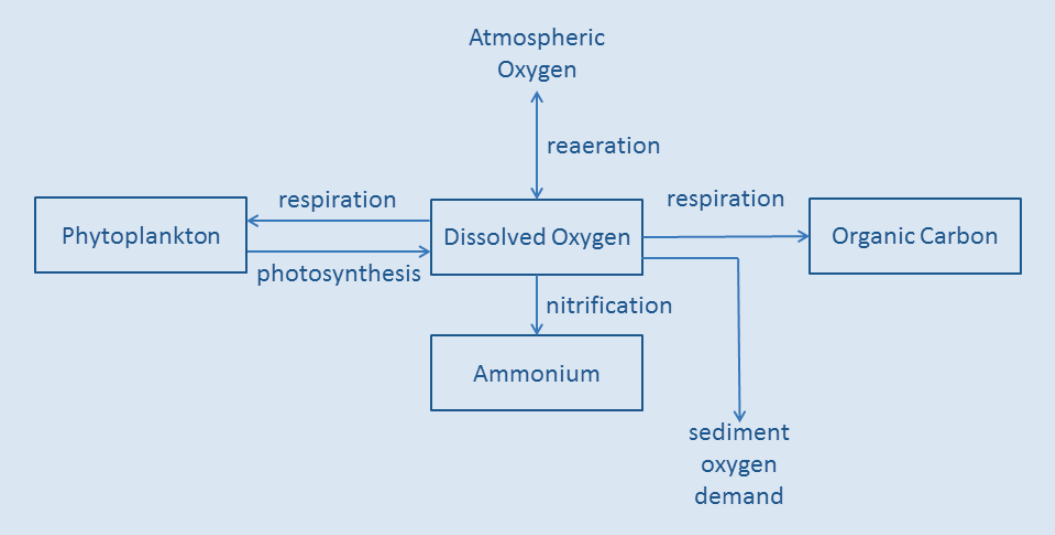

3.9.1 Reaeration

The rate of reaeration is proportional to the dissolved oxygen deficit in model segments which form the air-water interface:

$$\frac{\delta}{\delta t} DO = \frac{Kr}{\Delta z} \cdot (DOs - DO) \tag{36}$$

in which:

DO = dissolved oxygen concentration (g O_2 m^{-3})
Kr = reaeration coefficient (m d^{-1})
DOs = dissolved oxygen saturation concentration (g O_2 m^{-3})
Δz = model surface layer thickness (m).

In free-flowing streams, the reaeration coefficient depends largely on turbulence generated by bottom shear stress (O'Connor and Dobbins 1958). In lakes and coastal waters, however, wind effects dominate the reaeration process (O'Connor 1983). For the initial version of ICM-Lite, a relationship for wind-driven gas exchange (Hartman and Hammond 1985) is employed:

$$Kr = Arear \cdot Rnu \cdot Wms^{1.5} \tag{37}$$

in which:

$Arear$ = empirical constant (≈ 0.1)
Rnu = ratio of kinematic viscosity of pure water at 20 °C to kinematic viscosity of water at specified temperature and salinity
Wms = wind speed measured at 10 m above water surface (m s^{-1}).

Hartman and Hammond (1985) indicate *Arear* takes the value 0.157. In the present model, *Arear* is treated as a variable to allow for effects of wind sheltering, for differences in height of local wind observations, and for other factors. An empirical function that fits tabulated values of Rnu is

$$Rnu = 0.54 + 0.0233 \cdot T - 0.002 \cdot S \tag{38}$$

in which:

S = salinity (ppt)
T = temperature (°C).

Saturation dissolved oxygen concentration diminishes as temperature and salinity increase. An empirical formula that describes these effects (Genet et al. 1974) is

$$\begin{aligned} DOs = {} & 14.5532 - 0.38217 \cdot T + 0.0054258 \cdot T^2 \\ & - CL \cdot (1.665 \times 10^{-4} - 5.866 \times 10^{-6} \cdot T + 9.796 \times 10^{-8} \cdot T^2) \end{aligned} \tag{39}$$

in which:

CL = chloride concentration (= salinity/1.80655).

3.9.2 Mass balance equation for dissolved oxygen

The summary of all terms which affect dissolved oxygen is

$$\begin{aligned} \frac{\delta}{\delta t} DO = {} & AOCR \cdot \left[(1.3 - 0.3 \cdot PN) \cdot G - (1 - FC) \cdot R \right] \cdot B \\ & - FDOP \cdot (1 - FC) \cdot AOCR \cdot PR \\ & - AONT \cdot NT - \frac{DO}{KHr + DO} \cdot AOCR \cdot Korgc \cdot OrgC \\ & + \frac{Kr}{\Delta z} \cdot (DOs - DO) \end{aligned} \tag{40}$$

in which:

$AOCR$ = oxygen-to-carbon mass ratio in production and respiration (= 2.67 g O_2 g^{-1} C)
PN = algal ammonium preference ($0 \leq PN \leq 1$)
G = algal growth rate (d^{-1})
FC = fraction of algal and predator respiration released as $OrgC$ due to low DO concentration ($0 < FC < 1$)
R = algal respiration rate (d^{-1})
B = algal biomass (g m^{-3})
$FDOP$ = fraction of predation expressed as oxygen consumption ($0 < FDOP < 1$)
PR = predation on algae (g C m^{-3} d^{-1})
$AONT$ = oxygen consumed per mass ammonium nitrified (= 4.33 g O_2 g^{-1} N)
NT = nitrification rate (g N m^{-3} d^{-1})
KHr = dissolved oxygen concentration at which respiration of organic carbon is halved (g DO m^{-3})
$Korgc$ = respiration rate of $OrgC$ (d^{-1})
$OrgC$ = organic carbon (g m^{-3}).

3.10 User-defined substance

ICM-Lite provides a user-defined substance. Basic kinetics including first-order decay and settling are considered:

$$\frac{\delta}{\delta t}UDS = -Kuds \cdot UDS - Wuds\frac{\delta}{\delta z}UDS \tag{41}$$

in which:

UDS = user-defined substance (mass per unit volume)
$Kuds$ = decay rate (d^{-1})
$Wuds$ = settling rate (m d^{-1}).

The concentration of UDS will usually be g m^{-3}, consistent with most other model variables. The user can employ alternate units while taking care to employ consistent units for loads and boundary conditions.

4 Sediment-Water Interactions

Exchange of material between the water column and benthic sediments is an important component of aquatic ecosystems. Over lengthy time scales (e.g., years to decades), the sediments are an ultimate sink of nutrients and organic matter which settle from the water column. Over lesser time scales (e.g., seasons to years), however, sediment release of previously deposited nutrients can be a net source to the water column. Sediment oxygen demand may comprise a substantial fraction of total system oxygen consumption.

The complete CE-QUAL-ICM is usually executed in conjunction with a predictive sediment diagenesis model (DiToro 2001). The diagenesis model is demanding in terms of data requirements and is best implemented by the experienced user. As an alternative, ICM-Lite implements user-specified sediment-water nutrient and oxygen fluxes. Basic relationships are provided that express the influence of conditions in the water column on the specified fluxes.

User-specified fluxes are available for

- ammonium
- nitrate
- phosphate
- dissolved oxygen.

Transfer of particulate matter from water to sediments is treated through specification of a settling velocity. The model employs the convention that positive fluxes are from sediment to water and negative fluxes are from water to sediment. Fluxes of ammonium and phosphate are most often from sediments to water and are positive quantities. Nitrate commonly passes in both directions across the sediment-water interface and may be positive or negative. Since oxygen moves from water to sediments, sediment oxygen consumption is represented as a negative quantity.

4.1 Ammonium and phosphate

Sediment releases of ammonium and phosphate are specified at a reference temperature. The effect of temperature on release rate (Figure 15) is determined by an exponential relationship:

$$BEN = BENb \cdot e^{KS \cdot (T - TRben)} \tag{42}$$

in which:

BEN = sediment release at temperature T (g m^{-2} d^{-1})
$BENb$ = sediment release (g m^{-2} d^{-1}) specified at reference temperature $TRben$
KS = effect of temperature on sediment release ($C^{o\,-1}$)
T = temperature (C^{o}).

Figure 15. Effect of temperature on sediment-water fluxes, for three values of KS. When T = TRben, the flux equals the specified base value.

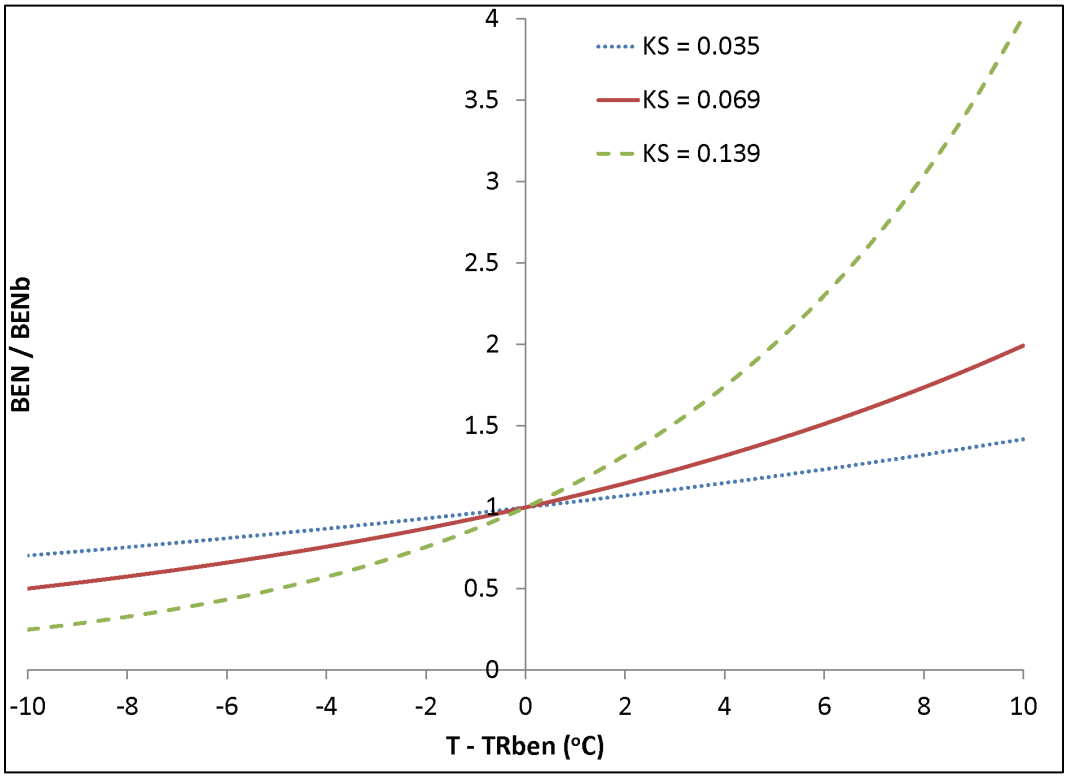

4.2 Nitrate

Movement of nitrate between water and sediments is strongly influenced by concentration of nitrate in the water column. When nitrate is abundant

in the water column, nitrate usually diffuses from overlying water into the sediments where it is denitrified to gaseous form. When nitrate is absent from the water column, small quantities of nitrate may diffuse from sediment interstitial water into the overlying water. The model allows for user-specified nitrate flux and provides a function (Figure 16) that relates flux to concentration:

$$BENNO_3 = BENNO_3b + MTC \cdot (SEDNO_3 - NO_3) \cdot e^{KS \cdot (T - TRben)} \quad (43)$$

in which:

$BENNO_3$ = sediment-water nitrate flux (g N m^{-2} d^{-1})
$BENNO_3b$ = specified sediment-water nitrate flux (g N m^{-2} d^{-1})
MTC = sediment-water mass transfer coefficient (m d^{-1})
$SEDNO_3$ = nitrate concentration in interstitial water (g m^{-3})
NO_3 = nitrate concentration in water overlying sediments (g m^{-3})

Figure 16. Effect of nitrate concentration in water column on sediment-water nitrate flux. Calculated for MTC = 0.1 m d^{-1}, SEDNO3 = 0.02 g m^{-3}. When NO_3 = $SEDNO_3$, the flux is zero.

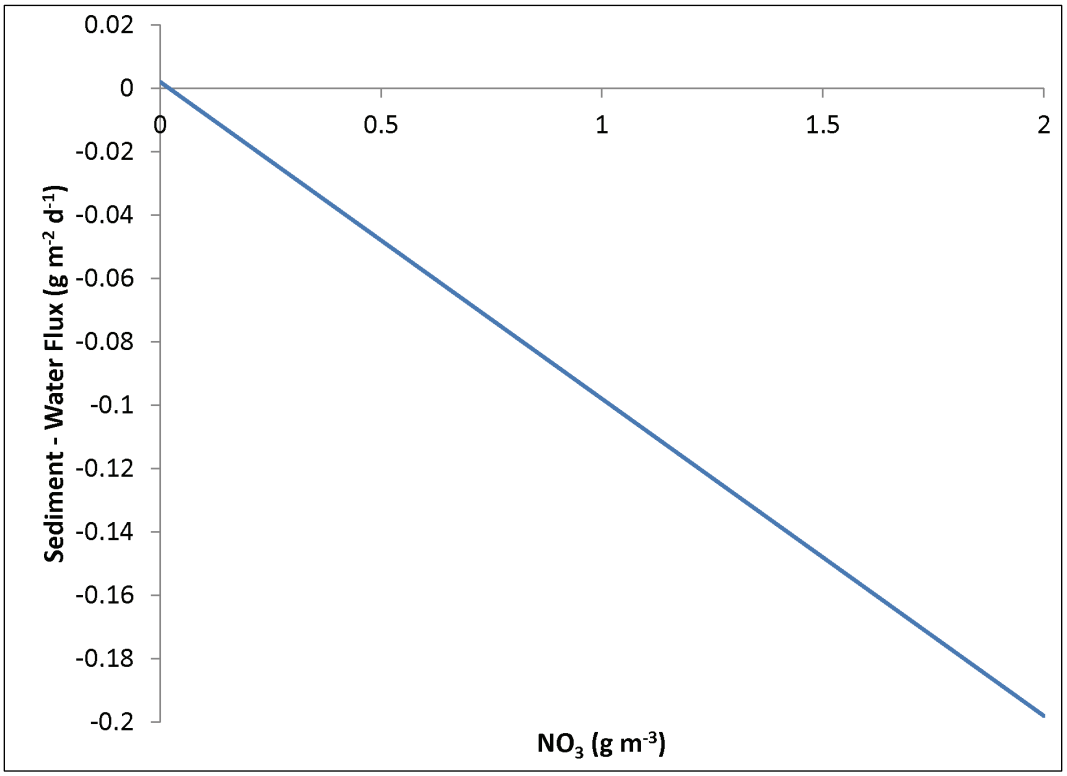

In model employment, the user specifies the nitrate flux, if known, or relies on the model to compute flux as a function of nitrate and temperature in the water column.

4.3 Sediment oxygen consumption

Oxygen consumption in the sediments depends upon water-column temperature and oxygen availability. As temperature increases, respiration in the sediment increases. Sediment oxygen consumption is reduced as oxygen concentration in the overlying water decreases (Figure 17). The model accounts for these influences through the relationship

$$BENDO = \frac{DO}{KHso + DO} \cdot BENDOb \cdot e^{KS \cdot (T - TRben)} \tag{44}$$

in which:

$BENDO$ = sediment oxygen consumption (g m^{-2} d^{-1})
$BENDO_b$ = sediment oxygen consumption under conditions of unlimited oxygen availability (g m^{-2} d^{-1}), specified at reference temperature $TRben$
$KHso$ = dissolved oxygen concentration at which sediment oxygen consumption is halved (g m^{-3}).

4.4 Parameter evaluation

Base fluxes and influences of temperature and other factors are best determined from observations collected in the prototype system. Table 1 lists observations from several systems that may be employed as starting values when no observations are available. Suggested starting values for parameters in the functions that relate sediment-water fluxes to conditions in the water column are listed in Table 2.

Figure 17. Effect of DO concentration on sediment oxygen consumption. Calculated for KHso = 1 g m^{-3}. When water column dissolved oxygen equals KHso, the sediment oxygen consumption is halved.

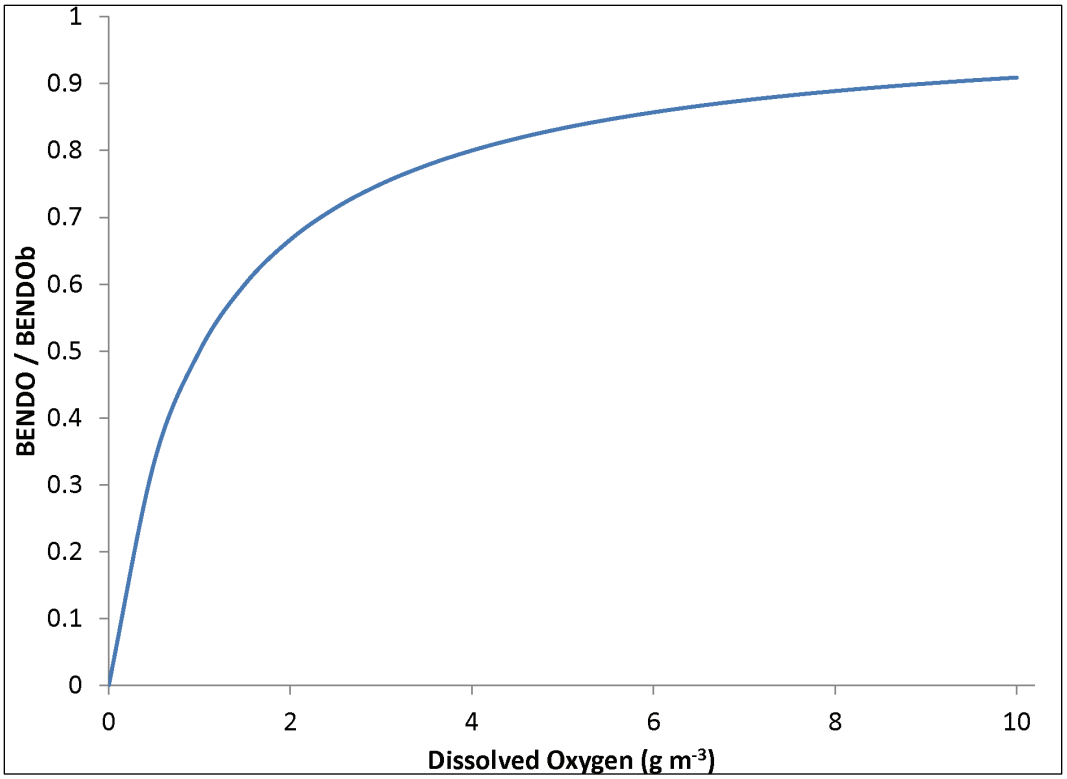

Table 1. Observed sediment-water fluxes.

Ammonium, g m^{-2} d^{-1}	Nitrate, g m^{-2} d^{-1}	Phosphate, g m^{-2} d^{-1}	SOD, g m^{-2} d^{-1}	System
0.01 to 0.28	-0.04 to 0.1	-0.003 to 0.03	-1.5 to -3.5	Chesapeake Bay (Boynton and Kemp 1985)
-0.001 to 0.09	-0.02 to 0.015	-0.007 to 0.031	-0.1 to -2.6	Narragansett Bay (Hale 1975)
0 to 0.15	0 to 0.002	-0.006 to 0.034	-0.6 to -2.4	Neuse and South Rivers, NC (Fisher et al. 1982)
-0.04 to 0.36	-0.1 to 0.08	-0.019 to 0.124	-0.1 to -2.7	Potomac Estuary (Callender and Hammond 1982)
-0.035 to 0.53	-0.23 to 0.03	0.001 to 0.22	-0.5 to -4.1	Patuxent Estuary (Boynton et al. 1980)

Table 2. Parameters in sediment-water flux relationships.

Parameter	Suggested Range
KS	0.04 to 0.07 $^{o}C^{-1}$
MTC	0.05 to 0.15 m d^{-1}
$SEDNO_3$	0 to 0.05 g m^{-3}
KHso	1 to 2 g m^{-3}

References

Boynton, W., and W. Kemp. 1985. Nutrient regeneration and oxygen consumption along an estuarine salinity gradient. *Marine Ecology Progress Series* 23:45–55.

Boynton, W., W. Kemp, and C. Osborne. 1980. Nutrient fluxes across the sediment-water interface in the turbid zone of a coastal plain estuary. In *Estuarine Perspectives*, ed. V. Kennedy, 93–110. New York: Academic Press.

Callender, E., and E. Hammond. 1982. Nutrient exchange across the sediment-water interface in the Potomac River Estuary. *Estuarine, Coastal and Shelf Science* 15:395–418.

Cerco, C., and M. Noel. 2004. Process-based primary production modeling in Chesapeake Bay. *Marine Ecology Progress Series* 282:45–58.

DiToro, D. 2001. *Sediment flux modeling*. New York: John Wiley and Sons.

Edinger, J., D. Brady, and J. Geyer. 1974. *Heat exchange and transport in the environment*. Report 14. Baltimore, MD: Department of Geography and Environmental Engineering, Johns Hopkins University.

Fisher, T., P. Carlson, and R. Barber. 1982. Sediment nutrient regeneration in three North Carolina estuaries. *Estuarine, Coastal and Shelf Science* 4:101–116.

Genet, L., D. Smith, and M. Sonnen. 1974. *Computer program documentation for the Dynamic Estuary Model*. Washington, DC: U.S. Environmental Protection Agency, Systems Development Branch.

Hale, S. 1975. The role of benthic communities in the nitrogen and phosphorus cycles of an estuary. *ERDA Symposium Series 1975*, 291–308.

Hartman, B., and D. Hammond. 1985. Gas exchange in San Francisco Bay. *Hydrobiologia* 129:59–68.

Jassby, A., and T. Platt. 1976. Mathematical formulation of the relationship between photosynthesis and light for phytoplankton. *Limnology and Oceanography* 21:540–547.

Leonard, B. 1979. A stable and accurate convection modelling procedure based on quadratic upstream interpolation. *Computer Methods in Applied Mechanics and Engineering* 19:59–98.

Monod, J. 1949. The growth of bacterial cultures. *Annual Review of Microbiology* 3:371–394.

O'Connor, D. 1983. Wind effects on gas-liquid transfer coefficients. *Journal of the Environmental Engineering Division* 190:731–752.

O'Connor, D., and W. Dobbins. 1958. Mechanisms of reaeration in natural streams. *Transactions of the American Society of Civil Engineers* 123:641–666.

Tchobanoglous, G., and E. Schroeder. 1987. *Water quality*. Reading, MA: Addison Wesley.

Thomann, R., and J. Fitzpatrick. 1982. *Calibration and verification of a mathematical model of the eutrophication of the Potomac Estuary*. Mahwah, NJ: HydroQual Inc.

Tuffey, T., J. Hunter, and V. Matulewich. 1974. Zones of nitrification. *Water Resources Bulletin* 10:555–564.

Walsh, M. 2012. Memorandum for major subordinate commands. February 8, 2012. Washington, DC: Headquarters, Department of the Army. http://planning.usace.army.mil/toolbox/library/MemosandLetters/USACE_CW_FeasibilityStudyProgramExecutionDelivery.pdf (accessed 16 April 2015).

Wezernak, C., and J. Gannon. 1968. Evaluation of nitrification in streams. *Journal of the Sanitary Engineering Division* 94(SA5):883–895.

REPORT DOCUMENTATION PAGE

Form Approved
OMB No. 0704-0188

1. REPORT DATE	2. REPORT TYPE	3. DATES COVERED *(From - To)*
July 2015	Technical Report	

4. TITLE AND SUBTITLE

Kinetics Formulations for ICM-Lite: A Tool to Predict and Quantify Ecosystem Benefits in Aquatic Systems

5a. CONTRACT NUMBER

5b. GRANT NUMBER

5c. PROGRAM ELEMENT NUMBER

6. AUTHOR(S)

Carl F. Cerco

5d. PROJECT NUMBER

5e. TASK NUMBER

5f. WORK UNIT NUMBER

7. PERFORMING ORGANIZATION NAME(S) AND ADDRESS(ES)

U.S. Army Engineer Research and Development Center
Environmental Laboratory
3909 Halls Ferry Road, Vicksburg MS, 39180-6199

8. PERFORMING ORGANIZATION REPORT NUMBER

ERDC/EL TR-15-8

9. SPONSORING/MONITORING AGENCY NAME(S) AND ADDRESS(ES)

Headquarters, U.S. Army Corps of Engineers
Washington DC 20314-1000

10. SPONSOR/MONITOR'S ACRONYM(S)

11. SPONSOR/MONITOR'S REPORT NUMBER(S)

12. DISTRIBUTION/AVAILABILITY STATEMENT

Approved for public release; distribution unlimited.

13. SUPPLEMENTARY NOTES

14. ABSTRACT

ICM-Lite is envisioned as a tool to rapidly predict and quantify ecosystem benefits in aquatic systems. ICM-Lite consists of three modules: a water quality module, a graphical user interface, and an ecosystems benefits module. This publication documents the formulations of the water quality module. Documentation includes the mass balance equation, kinetics in the water column, and representations of sediment-water fluxes. The mass balance relationships are intended to incorporate flows and volumes provided by the user and obtained outside of ICM-Lite. The kinetics include representations of the aquatic carbon, nitrogen, phosphorus, and oxygen cycles. Salinity, temperature, suspended solids, and one user-defined substances are included, as well. Sediment-water fluxes of organic matter, ammonium, nitrate, phosphate, and dissolved oxygen are considered.

15. SUBJECT TERMS

CE-QUAL-ICM model	Ecosystem benefit	Phosphorus
Dissolved oxygen	ICM-Lite model	Water quality
	Nitrogen	

16. SECURITY CLASSIFICATION OF:			17. LIMITATION OF ABSTRACT	18. NUMBER OF PAGES	19a. NAME OF RESPONSIBLE PERSON
a. REPORT	b. ABSTRACT	c. THIS PAGE			Carl F. Cerco
Unclassified	Unclassified	Unclassified	SAR	52	19b. TELEPHONE NUMBER *(Include area code)* 601-634-4207